Journal of Materials Chemistry B

Accepted Manuscript

ROYAL SOCIETY OF CHEMISTRY

www.rsc.org/materialsB

J. Mat. Chem. B

RSCPublishing

ARTICLE

Peptide modification of purified gellan gum

Cite this: DOI: 10.1039/x0xx00000x

C. J. Ferris,[† a,b] L. R. Stevens,[† a,b] K. J. Gilmore,[a] E. Mume,[c] I. Greguric,[c] D. M. Kirchmajer,[a,b] G. G. Wallace[a,*] and M. in het Panhuis[a,b *]

Received 00th January 2012,
Accepted 00th January 2012

DOI: 10.1039/x0xx00000x

www.rsc.org/

Gellan gum (GG) is an anionic polysaccharide with potential as a biopolymer for additive manufacturing (3D-bioprinting) and tissue engineering. Previous studies have shown GG to be highly cytocompatible, but lacking specific attachment sites required for anchorage-dependent cells. In this work, we modify purified-GG polymer with a short peptide containing the arginine-glycine-aspartic acid (RGD) sequence that is known to enhance integrin-mediated cell attachment. Radiolabelling of the peptide was used in optimisation of the conjugation procedure to achieve an overall efficiency of 40%. The purification of divalent cations from commercial GG samples was found to be critical for successful conjugation. Rheological studies revealed that the peptide coupling did not prevent gelation behaviour. C2C12 cells showed improved attachment on the surface of and encapsulated within RGD-GG hydrogels, differentiating to multinucleated myofibers after 5-7 days. PC12 cells showed minimal interactions with both GG and RGD-GG, with formation of cell clusters and impedance of terminal differentiation and neurite extension.

Introduction

The use of biopolymers that mimic the extracellular matrix to form scaffolds for cell culture is a well-established technique that has been employed over several decades. The more recent developments in additive manufacturing (or biofabrication), particularly 3D-bioprinting, have paved the way for the formation of complex tissue structures by layering cells and biomaterials in a spatially controlled manner[1]. In many cases however, biomaterials that are optimised for processing do not support cellular interactions and *vice versa*[2]. Most cell types are anchorage-dependent, and must anchor to a suitable substrate in order to facilitate normal behaviour[3, 4]. The creation of new materials that combine the support of correct cell behaviour with versatile processability will be key to realising the potential of biofabrication.

Gellan gum (GG) is an anionic polysaccharide comprised of a repeating tetramer, with one carboxylate functionality per repeat unit [5]. The structural and functional similarities between GG and the widely used alginate have helped identify it as a prime candidate for tissue engineering applications. The current uses and future potential of GG has been the focus of reviews in 2000[5] and 2013[6, 7] and several studies have demonstrated the processability and versatility of GG[7-9]. In particular, GG has been employed as a material for bio-printing of cells and cell-scaffolding structures [10-12]. The biocompatibility of GG has also been probed. Rat bone marrow cells[8], rabbit articular cartilage cells[13] and human chondrocytes[9] have all survived in GG, however these cell types are attachment-independent. Studies utilising anchorage-dependent cell lines have shown that GG is not an instructive cell encapsulation matrix. For example, fibroblasts[14] and oligodendrocytes[15] photo-encapsulated in methacrylated GG hydrogels maintained a non-responsive phenotype and showed reduced viability after several days in culture. Similar results have been obtained for analogous polysaccharide gel systems, with cardiomyocytes encapsulated in chitosan hydrogels[16] and endothelial cells encapsulated in alginate[17] showing a lack of cell adhesion. These results make it apparent that modification of GG hydrogels is required to support the adhesion, growth and normal function of anchorage-dependent cells.

The blending of complete proteins with polysaccharides is a popular approach for addressing this issue, as they contain the biofunctionality native to the extracellular matrix (ECM). Polysaccharides including alginate[18, 19], chitosan[20] and hyaluronic acid[21] have all been blended with collagen and/or laminin to create composite hydrogels that encourage the attachment and growth of encapsulated cells. Alternatively, polysaccharides may be directly functionalised to produce materials that combine both processability and cellular

attachment sites. The tri-peptide sequence arginine-glycine-aspartic acid (RGD) has been identified as the cell attachment site in many ECM proteins and is pivotal to integrin-mediated cell binding[22, 23]. This peptide, and other similar sequences, have been widely utilised to modify polymer biofunctionality[24]. One of the most common applications of this approach is the conjugation of RGD peptides to alginate[25]. Other research in this area involves modification of alginate with the peptide G_4RGDY, including a 6-month implantation study with a rat model, which showed good vascularisation and tissue integration *in vivo*[26]. The potential of RGD-alginates for injectable systems by delivering endothelial cells encapsulated in RGD-modified alginate *in vitro* has also been reported[17], while the potential of peptide-modified alginates for spinal cord repair has been demonstrated[27]. Human fibroblasts[28] and adipose derived stem cells[29] have also been incorporated into peptide-modified alginate gels. More recently, furan functionalisation of GG, followed by a Diels-Alder reaction with a synthetic variant of the GRDGS peptide was used to direct neural and mesenchymal stem cell differentiation with encouraging results[30, 31].

In this paper, we covalently linked unmodified peptides to GG, and monitored the reaction efficiency by tyrosine radiolabelling. The impact of RGD modification on GG's physical properties and cell interaction are presented.

Experimental

Gellan gum purification

All materials were obtained from Sigma, unless specifically stated otherwise. Commercial samples of low-acyl GG obtained from CP Kelco (traded as Gelzan™ CM) were purified to remove divalent cation using an established method[32-34]. A 1% (w/v) GG solution was formed by dissolving Gelzan™ CM (0.5 g) in 50 mL of hot Milli-Q water (60 °C, resistivity 18.2 MΩ cm). 1.25 g of Dowex 50W-X8 cation exchange resin (Fluka, H^+ form, 50-100 mesh), pre-rinsed in 1 M HCl and Milli-Q water, was then added and the hot mixture was stirred for 30 min to convert GG to the free acid form (gellanoic acid). The resin was allowed to settle and the supernatant decanted into a pre-heated beaker through a coarse filter. The resin was rinsed twice with small volumes of 60 °C water and added to the supernatant. To this solution (kept at ~ 60 °C), 4 M NaOH was added dropwise until the pH stabilised at ~ 7.5 to convert the gellanoic acid to the sodium salt (sodium gellanate, NaGG). After stirring for an additional 5 min, 100 mL of 2-propanol was added with continued stirring to precipitate a white fibrous product. This product was vacuum filtered, washed with 2-propanol and dried under vacuum overnight before being chopped into a fine powder and stored under cool, dry conditions until required.

Atomic absorption spectroscopy

The concentration of Na, Ca, K and Mg in GG and NaGG was determined using flame atomic absorption spectroscopy (AAS) burning acetylene/air. Samples were analysed using a Spectra AA 220FS (Varian) spectrometer equipped with sodium (589.6 nm), potassium (769.9 nm), calcium (422.7 nm) and magnesium (285.2 nm) hollow cathode lamp sources. Samples were prepared by digesting 1 g of dry material in 5 mL of hot concentrated sulphuric acid (Ajax Finechem), followed by dropwise addition of hydrogen peroxide (30% (v/v), Ajax Finechem) until the solution became transparent. The solution was allowed to cool prior to the addition of 16 mL of 12.6 mg/mL caesium chloride ionisation suppressant. The solution was then made up to 100 mL with the addition of Milli-Q H_2O and mixed thoroughly prior to measurement. Concentrations were blank-corrected and interpolated from calibration curves prepared using a certified multi-element standard solution (Inorganic Ventures). The limit of detection for each element was taken as twice the standard deviation of blank measurements.

RGD conjugation reaction

Peptides were coupled to NaGG using a wide variety of conditions. Under optimal conditions, 100 mg of NaGG was dissolved in a premade 50 mM solution of 2-(N-morpholino)ethanesulfonic acid (MES) buffer (pH 6.5) by stirring at ~60 °C to yield 10 mL of a 1 % (w/v) NaGG solution. In a separate vial, 1-ethyl-3-(3-dimethylaminopropyl) carbodiimide (EDC, Sigma) was added under N_2 gas and dissolved in MES buffer to yield a solution of 0.3 M EDC, 50 µL of which was immediately transferred to the NaGG solution. 50 µL of a 0.15 M solution of N-hydroxysulfosuccinimide (sulfo-NHS) in MES buffer was added to the reaction vessel. The solution was then vortexed and allowed to activate at 37 °C for 15 mins (Figure 1: Reactions 1,2). After activation, G_4RGDSY and G_4RGESY peptide (Auspep) solutions were added in sufficient quantity to bind to 1 mol% of total carboxylate groups and the mixtures (RGD-GG and RGE-GG, respectively) were retained overnight at 37 °C (Figure 1: reaction 3). A third mixture (GG/RGD) was prepared using a NaGG solution without addition of EDC, but coupled with 1 mol% G_4RGDSY.

After reaction, solutions were purified by dialysis against Milli-Q water over 5 days using Slide-a-Lyzer mini dialysis devices (0.1 mL, MWCO 10 kDa, ThermoScientific). The dialysed product was lyophilised for 2 days and then stored under cool (4 °C), dry (sealed in flask) conditions prior to use.

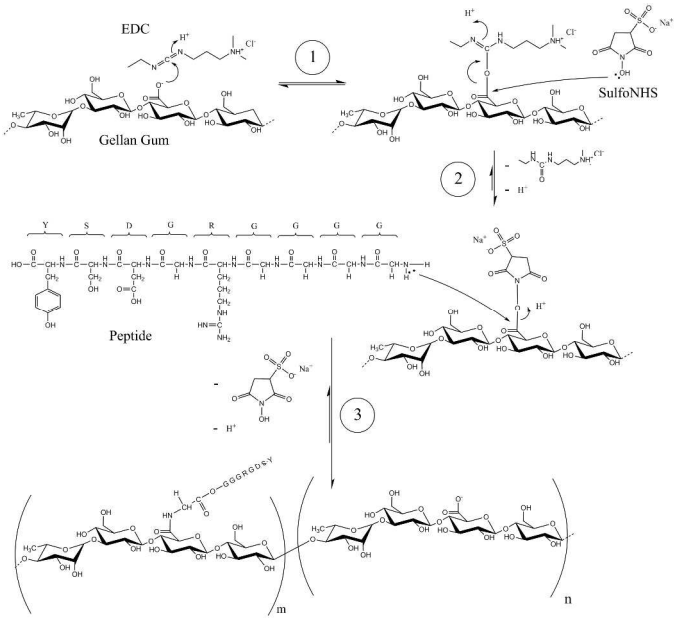

Figure 1: Reaction scheme for the peptide modification of purified GG, performed in three-steps: (1) EDC activation of the carboxylate on the GG backbone forming an unstable intermediate; (2) sulfo-NHS stabilisation of the reactive intermediate; and (3) peptide coupling to the GG backbone and regeneration of sulfo-NHS.

Radiolabelling to determine conjugation efficiency

For quantitative analysis of peptide binding to purified GG, the peptide G_4RGDSY was radiolabelled through radio-iodination of the tyrosine residue using the well-established chloramine-T method[35]. Iodine-125 carrier free radionuclide was purchased from Perkin-Elmer ($Na^{125}I$, $t_{1/2}$ = 59.4 days, NEZ033H010MC). 50 µL of a 1 mg/mL solution of G_4RGDSY in Milli-Q water was diluted with 180 µL of 0.1 M sodium phosphate buffer (pH 6.0). A 50 µL aliquot of $Na^{125}I$ (diluted 1:50 in 1 mM NaOH) was added, followed by 10 µL of 1 mg/mL chloramine-T in buffer. After 5 min, the reaction was quenched by the addition of 10 µL of sodium metabisulfite (Merck) at 2.5 mg/mL in buffer. The reaction mixture (300 µL total) was loaded onto an Oasis HLB SPE cartridge (Waters) that had been pre-equilibrated by eluting 5 mL methanol, 5 mL water and 10 mL 0.1% trifluoroacetic acid (TFA) in water (solvent A). The cartridge was then washed with 20 mL of solvent A to remove unbound iodine-125. Two fractions were eluted, the first with 4 mL of a 1:1 mixture of solvent A with 0.1% TFA in acetonitrile (solvent B), and the second with 4 mL of solvent B. The two fractions were pooled, dried in a rotary evaporator and re-dissolved in Milli-Q water (350 µL).

The concentration and purity of the radiolabelled peptide was confirmed by radio-HPLC analysis using a Shimadzu HPLC-DAD system equipped with an In/Us Systems gamma ram detector and an Eclipse XDB-C18 column (Agilent, 250x4.6 mm) with 5 µm particle size. Compounds were eluted using 30% (v/v) acetonitrile and water at a flow rate of 1 mL/min, isocratic, over 15 min. Peptide concentration was calculated using a calibration curve constructed from HPLC chromatograms of G_4RGDSY solutions of known concentration, plotting integrated peak area (λ = 254 nm) as a function of peptide concentration

Radiolabelled peptides were then coupled to NaGG as described above. Reaction products were separated using Zeba spin desalting columns (0.5 mL, MWCO 40 kDa, 50 °C ThermoScientific) to remove unconjugated peptide and other small reaction species from the peptide-conjugated NaGG. The radioactivity in all components of the system (i.e. sample, filtrates, eluates, dialysates, separation devices) was measured using a Perkin Elmer 2480 WIZARD^2 gamma counter and converted to specific activity by calibration against known samples of ^{125}I-G_4RGDSY. Conjugation efficiencies reported here are the ratios of specific activity in NaGG bound peptides, to the total activity recorded across all components.

Rheology

The rheological characteristics of GG, NaGG and RGD-GG hydrogels were investigated using an Anton Paar Physica MCR 301 rheometer equipped with a temperature controlled mantle and base plate. 1% (w/v) solutions of commercial GG, purified NaGG and modified RDG-GG were formed in Milli-Q water by stirring overnight at 50 °C. Viscosity was measured between 0.1 and 100 1/s shear rate at 37 °C.

The 1% (w/v) polymer solutions and two solutions of $CaCl_2$ with concentrations of 1% (w/v) and 0.9% (w/v), respectively were placed in a water bath at 80 °C. Receiving wells were formed from pre-cut cylinders of polyvinyl chloride (PVC) with internal diameter of 18 mm and height of 5 mm, which were placed in Petri dishes and sealed around the base with silicon sealant. 4.5 mL of each hot polymer solution was then mixed with 500 µL of $CaCl_2$ solution to yield final Ca^{2+} and polymer concentrations of 9 mM and 0.9% (w/v) respectively. NaGG and RGD-GG were mixed with 1% (w/v) $CaCl_2$, whilst commercial GG received 0.9% (w/v) $CaCl_2$ to adjust for the Ca^{2+} content already present in the material as determined by AAS (Table 1). Immediately after mixing, these solutions were pipetted into the PVC moulds and allowed to gel at 4 °C for 1 h. Once formed, hydrogels were transferred to the rheometer and equilibrated to 37 °C. Each hydrogel was slightly compressed using a 15 mm stainless steel parallel plate and tested under oscillating shear, with the strain amplitude rising from 0.01% to 100% shear strain at a constant angular frequency of 5 Hz.

Cell response

The phenotypic cell response to RGD-GG was assessed with the anchorage-dependent murine skeletal muscle C2C12 cell line and the neuronal rat pheochromocytoma PC12 cell line, both obtained from the American Type Culture Collection (ATCC). For surface seeding experiments, 0.15% (w/v) solutions of GG, GG/RGD, RGE-GG and RGD-GG were pipetted into 96-well plates and gelled by the slow addition of concentrated Dulbecco's Modified Eagle's Medium (DMEM,

Invitrogen) down the wall of the well. Hydrogels were then formed at 37 °C and equilibrated over 1 h using two changes of cell proliferation media (CPM), specifically DMEM (Invitrogen) supplemented with 10% (v/v) foetal bovine serum (FBS, Invitrogen) for C2C12 cells, and DMEM with 5% (v/v) FBS and 10% (v/v) horse serum for PC12 cells. Cells were seeded at 5000 cells/well and incubated at 37 °C and 5% (v/v) CO_2 with media changes every 2 days. Cell morphology was assessed daily using bright field microscopy, and cell viability was assessed using calcein AM (Molecular Probes, Life Technologies) and propidium iodide (PI) staining and fluorescence imaging for up to 6 days in culture. Differentiation was induced by switching to low serum media, i.e. DMEM with 2% (v/v) horse serum for C2C12 cells and DMEM with 1% (v/v) horse serum and 50 ng/mL nerve growth factor (NGF, Life Technologies) for PC12 cells. Differentiating cells were cultured for up to 6 days with media changes every 2 days.

Immunostaining was used to characterise the phenotype of differentiated C2C12 and PC12 cells. For C2C12 cells, staining targeted desmin, a sarcomeric intermediate filament protein expressed in skeletal muscle. For PC12 cells, staining targeted β-III tubulin, a globular microtubule protein expressed exclusively in neurons. In each case, cell nuclei were counter-stained using 4',6-diamidino-2-phenylindole (DAPI, 1 µg/mL), which binds strongly to DNA. Differentiated cells were fixed with 3.7% paraformaldehyde (PF, Fluka) in phosphate buffered saline (PBS) for 10 minutes at room temperature (21 °C, RT) and stored in PBS containing calcium and magnesium (DPBS) at 4° C prior to staining.

For staining of C2C12 cultures, cells were permeabilised with 50:50 methanol:acetone on ice for 5 minutes and washed with DPBS before blocking in 10% donkey serum (DS, Chemicon) with 0.05% Tween-20 (Sigma) for 1 hr at 21°C. Mouse monoclonal anti-desmin primary antibody (Novocastra) was diluted 1:100 in blocking solution and incubated at 4°C overnight. After two 10 min washes in DPBS, cells were incubated for 1 hr at 25˚C in the dark with the secondary antibody Alexa-546 donkey anti-mouse (Invitrogen) diluted 1:1000 in blocking solution. After two 10 min washes in DPBS, DAPI (Molecular Probes) was added at 1:1000 in DPBS for 5 min at 21 °C, before replacing with fresh DPBS and imaging using a Zeiss Axiovert inverted fluorescence microscope. For staining of PC12 cells, the same protocol was followed, however the primary antibody (anti-b-tubulin, Covance) was diluted 1:1000. Incubation times for all immunostaining reagants were doubled when cells were encapsulated in hydrogels rather than surface seeded.

For cell encapsulation studies sucrose was used to protect cells from any potential osmotic injury resulting from exposure to the hypotonic GG solution before addition of culture media. A GG solution at twice the desired final concentration was combined with an equal volume of a 20% (w/v) sucrose solution. This working solution was then used to resuspend cells that had previously been washed and suspended in 10% (w/v) sucrose at 5 x 10^5 – 2 x 10^6 cells/mL and pipetted into 96-well plates. CPM containing 5 mM $CaCl_2$ was then slowly added down the side of each well to crosslink the GG-cell suspensions. Media was changed twice over a period of 1 hr using CPM without additional $CaCl_2$, and cells were maintained and monitored over time in culture with media changes every 48 h.

MTS assays (Promega Corp.) were conducted according to the manufacturer's protocol on encapsulated C2C12 and PC12 cell cultures proliferating for periods up to 72 hr in NaGG and RGD-GG hydrogels at a polymer concentration of 0.15% (w/v).

Results and discussion

Gellan gum purification

The concentrations of major monovalent (Na^+, K^+) and divalent (Ca^{2+}, Mg^{2+}) cations in as-received (commercial) GG and purified NaGG were measured by atomic absorption spectroscopy (Table 1). Commercial samples of GG are predominantly in the potassium salt form, with lesser amounts of Na^+, Ca^{2+} and Mg^{2+} as the other major cations. The measured concentrations of divalent cations in commercial gellan gum were sufficient to neutralize around one-third of the carboxylate groups in GG, reducing their availability for reaction with EDC, and therefore the peptide.

To negate this impact, we purified our commercial GG samples (following a published procedure[32-34]) to remove divalent cations and yield monovalent cation salts. The product, sodium gellanate (NaGG), was a white fibrous product at ~ 60% yield by weight (Figure 2). The concentration of Na^+ in NaGG was equivalent to ~ 72.5 mol% of carboxyl groups. Hence, substantial percentages of the carboxylate sites were available for peptide coupling using the purified product. Additionally, In 2005, Ogawa et al. reported NaGG shifts from a random coil to a helixed state between 30-35˚C [36]. This transition is a key process in GG gellation and implies that NaGG will resist gellation at physiological temperature (37˚C) until divalent cations are added. The reduced prevelance of premature gellation allowed for thee dissolution of higher concentrations of GG at physiological temperatures, providing an additional avenue for improving the reaction efficiency in EDC-mediated peptide conjugation.

Table 1: Concentration of major cations present in as-received (commercial) gellan gum (GG) and purified sodium gellanate (NaGG), measured by atomic absorption spectroscopy.

Element (% w/w)	Na^+	K^+	Ca^{2+}	Mg^{2+}
GG	0.6 ± 0.1	4.5 ± 0.2	1.2 ± 0.1	0.11 ± 0.01
NaGG	2.5 ± 0.1	1.0 ± 0.1	< 0.06	< 0.03

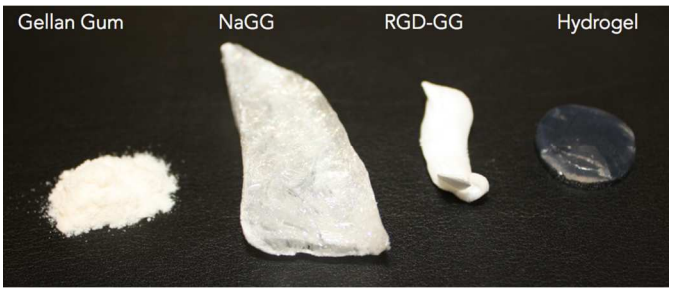

Figure 2: Gellan gum (GG) through each stage of processing. From left to right, as-received (commercial) GG powder, lyophilised NaGG, lyophilised RGD-GG and a 0.9% (w/v) RGD-GG hydrogel.

Peptide conjugation to purified GG

Conjugation reactions with NaGG were performed under a range of conditions including variations to peptide, NaGG, EDC and sulfo-NHS concentrations, temperature, and reaction buffer (Table 2, Figure 3). Conjugation of 0.1% (w/v) NaGG solutions yielded an efficiency (~ 19%) which was significantly higher than those obtained using commercial GG (<5%, see the Electronic Supporting Information) under the same conditions.

This clearly indicates that the removal of divalent cation (present in commercial GG) significantly enhanced the conjugation efficiency without any additional optimisation of the reaction. The purification process also afforded better control of the gellation process of GG, and enabled conjugation reactions using more concentrated 0.5% (w/v) and 1.0% (w/v) NaGG solutions, yielding efficiencies of around 35%.

Based on the data (Table 2, Figure 3) obtained through radiolabelling, selection of buffer, pH and adequate concentrations of EDC and GG appear to be the primary determinants of conjugation efficiency. MES buffer at pH 6.5 was found to significantly out-perform the other tested systems, however the same buffer at pH 5 yielded no significant peptide conjugation. These results suggest that a pH of 6.5 achieved a balance between the reactivity of the EDC, the terminal amine of the peptide and the carboxyl group on the polymer, a finding similar to results obtained for alginate.[25].

A pH of 6.5 strikes a balance between EDC's peak reactivity at pH ~4.5, and that of the terminal amine, which is strongly activated at pH 8-9[24]. The GG pKa value of 3.06 implies that a pH of 6.5 promotes dissociation in over 99.9% of available carboxylate residues[37]. However, despite the similar pH value (6.7) the sodium acetate buffer impeded RGD peptide coupling, possibly due to de-activation of EDC by nucleophilic attack from acetate ions[38], underscoring the importance of appropriate buffer selection.

Table 2: Reaction efficiencies for the EDC-mediated conjugation of G_4RGDSY to NaGG under varying reaction conditions. Reaction efficiencies were determined by gamma counting of conjugated and radio-labelled G_4RGDSY after separation of unbound peptide by spin desalting.

NaGG (% w/v)	EDC ($\%_{COOH}$)	G_4RGDSY ($\%_{COOH}$)	Temp (˚C)	Buffer	Efficiency (% ±1 STD)
1	20	2	37	MES $^{pH\ 6.5}$	37.0 ± 1.0
1	20	0.2	37	MES $^{pH\ 6.5}$	37.8 ± 3.0
1	20	0.02	37	MES $^{pH\ 6.5}$	30.9 ± 3.1
1	10	2	37	MES $^{pH\ 6.5}$	33.3 ± 2.8
1	5	2	37	MES $^{pH\ 6.5}$	24.4 ± 3.1
1	20	2	21	MES $^{pH\ 6.5}$	35.2 ± 0.3
1	20	2	60	MES $^{pH\ 6.5}$	26.9 ± 2.3
1	0	2	37	MES $^{pH\ 6.5}$	9.7 ± 0.6
0.5	20	2	37	MES $^{pH\ 6.5}$	35.3 ± 0.4
0.1	20	2	37	MES $^{pH\ 6.5}$	18.7 ± 0.7
1	20	2	37	MES $^{pH\ 5.0}$	9.92 ± 0.8
1	20	2	37	Na_3PO_4 $^{pH\ 8.0}$	15.1 ± 0.3
1	20	2	37	$NaC_2H_3O_2$ $^{pH\ 6.7}$	13.7 ± 1.1
1	20	2	37	Milli-Q H_2O	11.8 ± 0.8

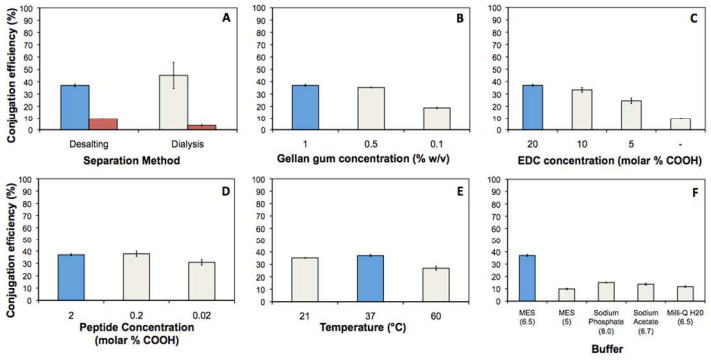

Figure 3: Peptide (G_4RGDSY) conjugation efficiencies as determined after HPLC by gamma counting of radio-labelled iodine on the terminal tyrosine of the G_4RGDSY peptide. Efficiencies were compared in terms of separation method (A), NaGG concentration (B), EDC concentration (C), peptide concentration (D), reaction temperature (E) and buffer selection (F). Blue shaded data indicate the conditions that were carried across to the other reactions shown, white bars indicate the additional tested conditions. Red bars in (A) represent control reactions with no added EDC. Error bars represent 1 standard deviation of the mean.

The EDC concentration was varied from 0-20 mol% of available carboxylate groups, with reaction efficiencies rising four fold over that range. This result is similar to that previously observed for alginate[25], i.e. peak efficiency at an EDC concentration of 10% of available carboxylate groups. EDC concentrations above 20% were not employed to minimise a previously reported side reaction in which the active ester undergoes internal rearrangement and incorporates into the product[25, 39]. It is suggested that in the absence of EDC, the apparent conjugation efficiency of 10% can be attributed to the presence of unbound RGD peptide (remaining after a single spin-desalting step). Thorough purification by five-day dialysis was observed to better separate unbound peptide (Figure 3A).

Ambient (21 ˚C) and physiological (37 ˚C) temperatures were found to promote conjugation equally well (Figure 3E). However elevated temperatures (~60 ˚C) were found to reduce conjugation efficiency. It is likely that this is related to a trade-off between reaction kinetics of EDC coupling and the

availability of carboxyl groups for activation. The input concentration of G_4RGDSY peptide (when varied over 3 orders of magnitude) was not observed to significantly alter the overall conjugation efficiency (Figure 3D).

These results suggest that RGD-peptide density could be tailored to suit a wide variety of extracellular environments. The density of RGD peptides presented to cells has been shown to affect a range of cellular responses including attachment, spreading, proliferation and differentiation[24, 40-42].

The highest efficiency for conjugation of G_4RGDSY to NaGG achieved in this work (~ 40%) was lower than that observed by for the conjugation of GRGDY to alginate (> 80%) [25]. The lower efficiency could be due to the use of a longer peptide sequence. This is supported by a subsequent report demonstrating that a longer peptide G_4RGDY conjugated to alginate resulted in a decrease in efficiency to 55%[42].

For our work, we chose to use an RGD-containing peptide with a poly-glycine tail due to evidence from several studies indicating the need for a spacer that separates the RGD sequence from the material to which it is conjugated, enhancing its availability to cellular integrins[24]. The required length of this spacer, or the need for one at all, is largely dependent upon the structure of the host material. We were therefore guided by work characterising the effect of glycine tail length on the response of human fibroblast cells to RGD-modified alginate hydrogels[28]. In this report, it was shown that a minimum spacer length of four glycine units was required to facilitate the development of focal adhesions, cell proliferation and a reduction in cell stress markers. The apparent trade-off between reaction efficiency, optimal with short peptides, and cellular response, favouring longer peptides, is an observation that warrants investigation with respect to all RGD-modified polymers.

Impact of RGD-modification on the rheological behaviour of GG

One of the key benefits of GG as a biomaterial is its mechanical and rheological behaviour. Specifically, GG forms self-supporting hydrogels under physiologically relevant conditions, but flows freely when no divalent cations are present [43]. This behaviour is mediated by inter-chain helix formation, which is stabilised by the ionic bridging of neighbouring carboxylate residues by cations, particularly Ca^{2+} [44]. Modification of GG, particularly when involving the carboxylate groups, has the potential to disrupt this behaviour. Rheological testing was performed to quantify the impact of peptide modification on the physical properties of GG. The flow curves of the solutions of as-received GG and its derivatives (prior to crosslinking) showed that as-received GG exhibited higher apparent viscosity values compared with purified NaGG and RGD-GG (Figure S1, the Electronic Supporting Information, ESI).

Oscillating shear dynamic mechanical analysis was performed on hydrogels of 0.9% (w/v) as-received GG with 9 μM $CaCl_2$ (Figure 4). Storage modulus (G') and loss modulus (G") are measures of the elastic and viscous behaviours of non-Newtonian materials, respectively. All tested hydrogels exhibited linear viscoelastic (LVE) regions in which G' and G" were invariant with strain. The dominance of G' over G" in this region is indicative of fully formed, pseudo-solid hydrogels.

The significant reduction in G' and G" values for RGD-GG compared to NaGG indicates a generalised weakening of inter-chain interactions has resulted from the peptide modification reaction. The magnitude of this effect is notable given that only ~1 mol% of available carboxylate residues were modified with G_4RGDSY, yet the reduction in G' and G" was between 1-2 orders of magnitude. This suggests that the peptide alters GG rheological characteristics in a manner that cannot be singularly explained by a reduced availability of carboxylate groups. We propose that the bulky peptide hinders the formation of inter-chain helicies between adjacent GG chains, which typically precedes ionic cross-linking[43]. Importantly, the rheological characterisation has demonstrated that peptide conjugation does not prevent gellan gum's gelation behaviour that is so critical to many applications in tissue engineering and additive manufacturing (although weaker gels are formed).

Table 3: Linear viscoelastic (LVE) region in terms of storage (G') and loss (G") moduli of hydrogels formed from commercial (GG), purifed (NaGG) and RGD-modified (RGD-GG) gellan gum. The end point of the LVE reported here is taken to be the onset of a sustained rise in the loss modulus, typically around 0.5% strain.

	GG	NaGG	RGD-GG
LVE G' (kPa)	105 ± 35.3	85.9 ± 6.0	5.64 ± 0.37
LVE G" (kPa)	10.0 ± 0.32	4.5 ± 1.3	0.37 ± 0.15
End LVE (Strain %)	0.21 ± 0.06	0.35 ± 0.12	0.82 ± 0.51

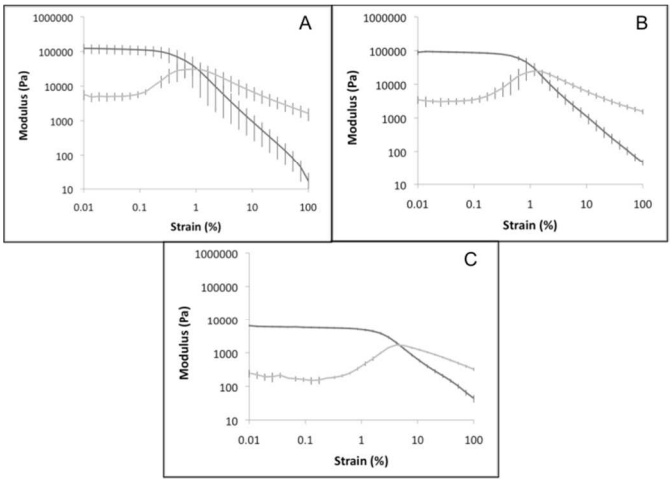

Figure 4: Oscillatory shear rheometry, sweeping shear strains from 0.01-100% at 37°C. Tests were performed on 10 mm x 17 mm hydrogel cylinders comprising 9 mM $CaCl_2$ and 0.9% (w/v) of A: commercial GG, B: purified NaGG and C: peptide modified RGD-GG.

Cell response to peptide-modified gellan gum

We investigated the response of two cell lines to RGD-GG, the murine skeletal muscle C2C12 cell line which is anchorage-dependent, and the rat pheochromocytoma PC12 cell line, which exists as both adherent and suspended populations in standard tissue culture on polystyrene. After initial optimisation of the concentration of NaGG for cell surface seeding, these cells were seeded both on the surface of, and encapsulated within, 0.15% (w/v) NaGG and 0.15% (w/v) RGD-GG hydrogels with the peptide coupled at 0.1 mol% and 1 mol% of available carboxyl groups, denoted as RGD-GG(0.1%) and RGD-GG(1.0%). The RGD-peptide concentration in the latter hydrogels is approximately 9 µmol/L, with an effective surface availability of approximately 4.5 fmol/cm^2, calculated using the established methods[42,24].

In order to rule out that any changes to cell response could be due to changes in the physical characteristics of the hydrogel rather than as a result of specific integrin-mediated interactions with the RGD peptide, control samples of NaGG were conjugated with the peptide G_4RGESY at 1 mol%, denoted RGE-GG(1%). The RGE sequence differs chemically from the RGD sequence by only one –CH_2 group, however this minor change has a significant effect on its integrin affinity, which is several orders of magnitude lower than for RGD[45]. An additional hydrogel control sample was prepared using a mixture of NaGG (without added EDC) and 1 mol% G_4RGDSY, denoted GG/RGD. As the RGD is not conjugated, but non-specifically bound to GG, there is a lower amount of peptide remaining due to the dialysis procedure (Figure 3A).

Figure 5 shows cells seeded on the surface of 0.15% (w/v) RGD-GG hydrogels and 0.15% (w/v) NaGG controls after 24 h in culture. Cells on unmodified NaGG surfaces formed large aggregates typical of poor adhesion to the substrates. Cells formed similar aggregates on RGE-GG(1%) indicating that conjugation of this non-integrin-targeting sequence did not modify cell attachment to the surface. On GG/RGD, the hydrogel containing non-specifically bound peptide, cell aggregates were smaller but there was little evidence of cell spreading.

On the surface of RGD-GG(1%) hydrogels however, C2C12 cells were observed to rapidly attach, and few large cell clusters were observed. After 24 h of culture, C2C12 cells exhibited a typically flattened and elongated morphology, indicating the development of strong cell adhesions and implicating specific integrin-mediated interaction. C2C12 cell attachment was dependent on RGD density, as cells seeded on hydrogels with a lower concentration of RGD peptide, RGD-GG(0.1%), adopted a rounded morphology or formed small aggregates with few flattened and elongated cells (Figure 5E). PC12 cells retained rounded morphologies typical of this cell line under proliferation conditions (data not shown).

C2C12 cells encapsulated in peptide-modified and control hydrogels (Figure 5F-J) showed a similar range of responses to those seeded on corresponding hydrogel surfaces. Cells in NaGG maintained a rounded morphology reflective of a lack of adhesive interactions (Figure 5F). A similar response was observed for cells encapsulated in RGE-GG(1%) (Figure 5G) and GG/RGD (Figure 5H) hydrogels, in agreement with surface-seeded results. RGD-GG(1%) hydrogels, however, supported the attachment and proliferation of encapsulated C2C12 cells (Figure 5I). This effect was observed to a lesser extent for the lower peptide density hydrogel formed using RGD-GG(0.1%) (Figure 5J). PC12 cells, in contrast, showed minimal change in morphology resulting from the presence of RGD, with the majority of cells remaining in clusters independent of the presence of RGD-peptide (Figure S2, ESI).

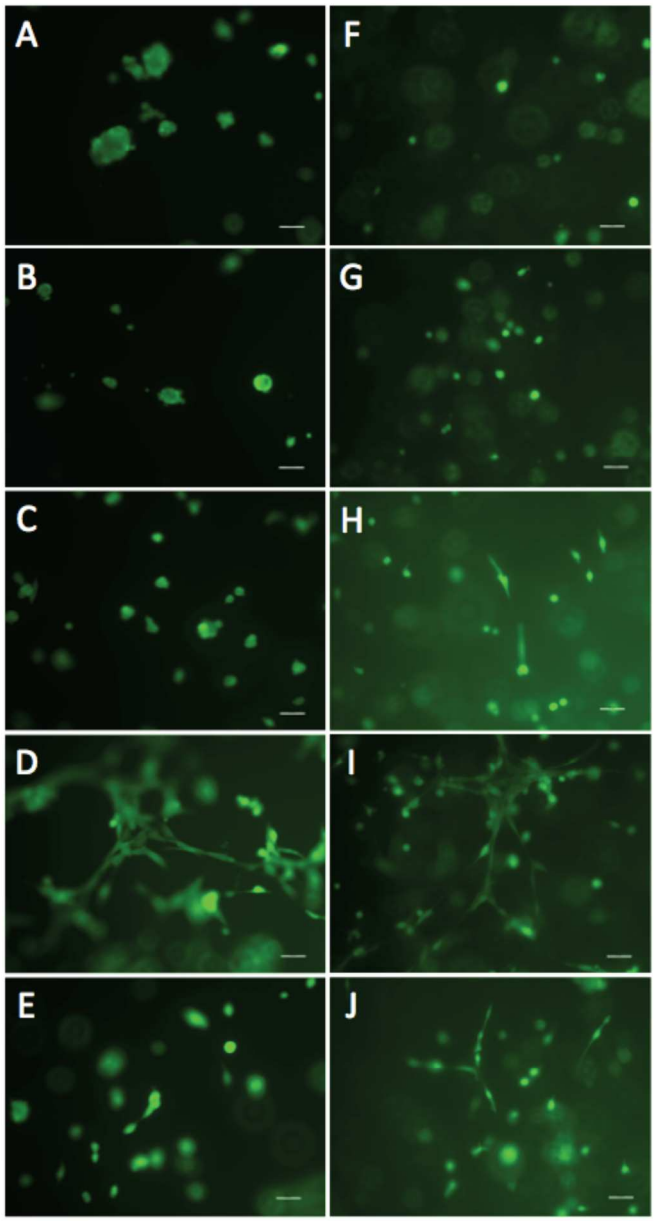

Figure 5: C2C12 cells seeded on the surface of (A-E) and encapsulated within (F-J) 0.15% (w/v) hydrogels after 24 h under proliferation

conditions. Hydrogels were formed from unmodified NaGG (A, F), RGE-GG(1%) (B, G), GG/RGD (C,H), RGD-GG(1%) (D, I), RGD-GG(0.1%) (E, J). Scale bars represent 50 µm.

Both C2C12 and PC12 cells were observed to proliferate when surface seeded or encapsulated within the RGD-GG(1.0%) gels. MTS assays were used to quantify changes in the cellular metabolic activity of encapsulated cells, which can be related to changes in cell number or activity within the cell population. MTS assays applied to GG encapsulated PC12 and C2C12 cells showed that the overall metabolic activity was greater for cells encapsulated in 0.15% (w/v) RGD-GG(1.0%) hydrogels than in the equivalent NaGG hydrogels.

For PC12 cells there was a consistent increase in metabolic activity over a 72 h period that reflected the observed proliferation of encapsulated cells (Figure 6A). For C2C12 cells, the increase in metabolic activity was consistently delayed (Figure 6B). However, at alltime points the cellular metabolic activity in RGD-GG(1.0%) gels was higher than that in the corresponding NaGG gels, indicating that the RGD peptide afforded a better growth environment to both of the cell lines over a 72 h culture period.

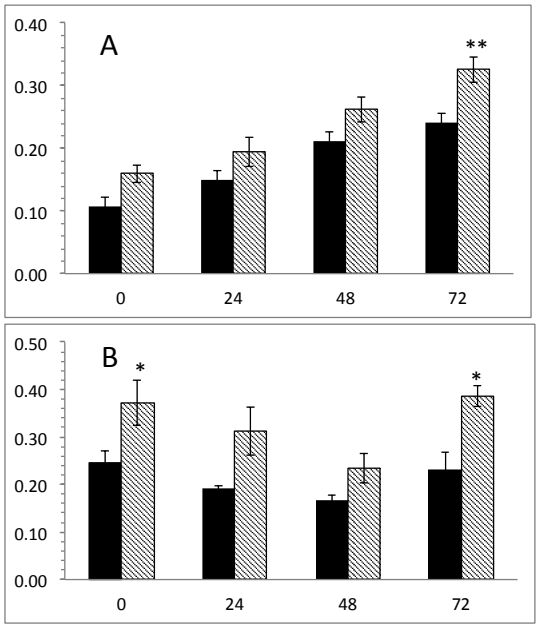

Figure 6: MTS assays for encapsulated PC12 (A) and C2C12 (B) cells under proliferative conditions over a 72 h period. Grey and black bars indicate 0.15% (w/v) hydrogels formed using RGD-GG(1.0%) and NaGG, respectively. The increased metabolic activity in cells encapsulated in RGD-GG was statistically significant at the **99% or *97% confidence level (Student's T test).

Both encapsulated and surface-seeded cells were induced to differentiate by exposure to low serum conditions. After only 12 h, C2C12 cells on the surface of RGD-GG had formed into large multi-cellular fibres and aggregates, and this contraction continued with further culture. C2C12 cells cultured on polystyrene take up to 6 days to differentiate, however early differentiation has previously been observed for C2C12 cells on the surface of RGD-alginate hydrogels[25]. This was attributed to the compliant nature of the hydrogel substrate, and could be the reason for the rapid cell response observed in the current work.

After 5 days incubation under differentiation conditions, fixed and immunostained samples showed formation of multinucleated myofibres, typical of differentiated skeletal muscle (Figure 7A). Encapsulated C2C12 cells were also found to differentiate into multinucleated skeletal muscle fibres within RGD-GG(1.0%) hydrogels (Figure 7B-C), in contrast to the cell behaviour observed within gels prepared without the peptide (Figure 7D). The extent of multinuclear fibre formation was found to be dependant on the encapsulated cell density, i.e. at higher cells density ($2x10^6$ cells/mL) a higher percentage of cells were incorporated into fibres than at lower density ($0.5x10^6$ cells/mL). This behaviour corresponds to the observed role of skeletal muscle cell density culture.

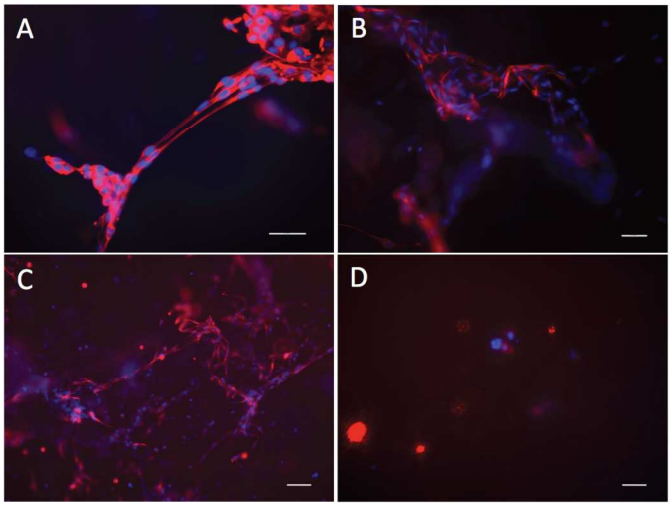

Figure 7: (A) Surface seeded and (B, C) encapsulated C2C12 cells after 5 days of culture in 0.15% (w/v) RGD-GG(1.0%) hydrogels under differentiation conditions. (D) Encapsulated C2C12 cells after 5 days of culture in 0.15% (w/v) NaGG hydrogels under differentiation conditions. Cells were immunostained for the skeletal muscle protein desmin (red) and nuclei stained with DAPI (blue). Scale bars represent 50 µm.

In contrast, assessing the differentiation of PC12 cells within RGD-GG(1.0%) and NaGG hydrogels was problematic as cells readily clustered in both materials. Neurite extension was observed only for single cells or very small clusters (Figure S2, ESI). Differentiation from larger cell clusters was impeded, suggesting that the RGD density and/or GG concentration may need to be further optimised for this cell type to achieve improved cell differentiation. Our results for PC12 cells are in agreement with previous studies on RGD-functionalised cell culture plastic surfaces that showed that PC12 cells exhibited enhancement in proliferation without significant morphological changes[46, 47]. More recent work however has identified an important role in local microstructure for controlling cell behaviour[48], and PC12 and C2C12 cells on RGD-modified

surfaces showed differing behaviour depending on the microstructure employed [49, 50]. In a similar manner, the local density of RGD sites appears to play a significant role in controlling the behaviour of attached cells[41,42]. In addition, mechanical properties are known to impact cell behaviour [51], and the fusion of C2C12 cells into myofibres has been shown to be dependent on the mechanical properties of their environment[52].

In summary, we observed adhesion, spreading, proliferation and differentiation into multinucleated fibres for C2C12 cells, however PC12 cells showed enhancement only in overall metabolic activity, broadly in line with previous findings[41, 42, 46, 47]. Realising the potential of any material for tissue engineering inevitably relies on tailoring its mechanical and biochemical properties to match that of the target tissue. The tuneable mechanical properties of GG [53, 54], and capacity for peptide functionalisation, make it an excellent candidate for this role.

Conclusions

We have presented a covalent modification procedure for the conjugation of short peptides to gellan gum. Purification of GG was essential for successful conjugation, and optimisation of coupling conditions resulted in a conjugation efficiency of ~40%. Rheological studies indicated that the attachment of RGD to the carboxyl residues does not impede the formation of hydrogels, although mechanical weaker gels are formed.

C2C12 and PC12 cell lines proliferated when seeded on the surface and encapsulated into the gels and the increase in overall cellular metabolic activity in RGD-GG hydrogels was quantitated by MTS assay. The differentiation of the C2C12 cell line was enhanced by the RGD-peptide for both surface seeded and encapsulated cells, resulting in multinucleated skeletal muscle fibres either on the gel surface or throughout the bulk of RGD-GG hydrogels.

This paper provides a reliable method for the functionalisation of GG with short peptide sequences, with the covalent linkage of G_4RGDSY found to produce a significant improvement to the cell attachment properties of GG. It is anticipated that the reported enhancement in cell interactions will increase the use of GG as a cell scaffolding biomaterial for tissue engineering and a bio-ink for additive manufacturing (3D-bioprinting).

Acknowledgements

The authors wish to acknowledge the material and financial support provided by the University of Wollongong (UOW), the Australian Institute of Nuclear Science and Engineering (AINSE) the Australian Research Council (ARC) through its Centre of Excellence, Laureate and Future Fellowship programs. Mr R. Clark (CP Kelco) is thanked for stimulating discussions.

Notes and references

† Co-first authorship: C. J. Ferris and L. R. Stevens contributed equally to this work.

[a]Intelligent Polymer Research Institute, ARC Centre of Excellence for Electromaterials Science, University of Wollongong, NSW 2522, Australia.

[b]Soft Materials Group, School of Chemistry, University of Wollongong, Wollongong, NSW 2522, Australia.

[c]Australian Nuclear Science and Technology Organisation, Lucas Heights, NSW 2234, Australia.

* Authors to whom correspondence should be addressed. E-mail: gwallace@uow.edu.au, panhuis@uow.edu.au.

Electronic Supplementary Information (ESI) available: peptide conjugation to as-received (commercial) gellan gum, flow curves and cell imaging. See DOI: 10.1039/b000000x/

1. F. P. W. Melchels, M. A. N. Domingos, T. J. Klein, J. Malda, P. J. Bartolo and D. W. Hutmacher, *Prog. Polym. Sci.*, 2012, **37**, 1079-1104.
2. J. Malda, J. Visser, F. P. Melchels, T. Jungst, W. E. Hennink, W. J. Dhert, J. Groll and D. W. Hutmacher, *Adv. Mater.*, 2013, **25**, 5011-5028.
3. A. P. Gilmore, *Cell Death Differ.*, 2005, **12 Suppl 2**, 1473-1477.
4. S. Frisch and H. Francis, *J Cell Biol.*, 1994, **124**, 619-626.
5. I. Giavasis, L. Harvey and B. McNeil, *Crit. Rev. Biotechnol.*, 2000, **20**, 177-211.
6. V. D. Prajapati, G. K. Jani, B. S. Zala and T. A. Khutliwala, *Carbohydr. Polym.*, 2013, **93**, 670-678.
7. C. J. Ferris, K. J. Gilmore, G. G. Wallace and M. i. h. Panhuis, *Soft Matter*, 2013, **9**, 3705.
8. A. M. Smith, R. M. Shelton, Y. Perrie and J. J. Harris, *J. Biomater. Appl.*, 2007, **22**, 241-254.
9. J. T. Oliveira, L. Martins, R. Picciochi, P. B. Malafaya, R. A. Sousa, N. M. Neves, J. F. Mano and R. L. Reis, *J. Biomed. Mater. Res. A*, 2010, **93**, 852-863.
10. R. Levato, J. Visser, J. A. Planell, E. Engel, J. Malda and M. A. Mateos-Timoneda, *Biofabrication*, 2014, **6**, 035020.
11. C. J. Ferris, K. J. Gilmore, S. Beirne, D. McCallum, G. G. Wallace and M. in het Panhuis, *Biomater. Sci.*, 2013, **1**, 224.
12. J. Visser, B. Peters, T. J. Burger, J. Boomstra, W. J. Dhert, F. P. Melchels and J. Malda, *Biofabrication*, 2013, **5**, 035007.
13. J. T. Oliveira, L. S. Gardel, T. Rada, L. Martins, M. E. Gomes and R. L. Reis, *J. Orthop. Res.*, 2010, **28**, 1193-1199.
14. D. F. Coutinho, A. F. Ahari, N. N. Kachouie, M. E. Gomes, N. M. Neves, R. L. Reis and A. Khademhosseini, *Biofabrication*, 2012, **4**, 035003.
15. N. A. Silva, A. J. Salgado, R. A. Sousa, J. T. Oliveira, A. J. Pedro, H. Leite-Almeida, R. Cerqueira, A. Almeida, F. Mastronardi, J. F. Mano, N. M. Neves, N. Sousa and R. L. Reis, *Tissue Eng. A*, 2010, **16**, 45-54.
16. F. Rask, A. Mihic, L. Reis, S. M. Dallabrida, N. S. Ismail, K. Sider, C. A. Simmons, M. A. Rupnick, R. D. Weisel, R.-K. Li and M. Radisic, *Soft Matter*, 2010, **6**, 5089.
17. S. J. Bidarra, C. C. Barrias, K. B. Fonseca, M. A. Barbosa, R. A. Soares and P. L. Granja, *Biomaterials*, 2011, **32**, 7897-7904.
18. K. Y. Lee and D. J. Mooney, *Prog. Polym. Sci.*, 2012, **37**, 106-126.
19. J. Sun, W. Xiao, Y. Tang, K. Li and H. Fan, *Soft Matter*, 2012, **8**, 2398.
20. L. A. Reis, L. L. Chiu, Y. Liang, K. Hyunh, A. Momen and M. Radisic, *Acta Biomater.*, 2012, **8**, 1022-1036.
21. S. Suri and C. Schmidt, *Tissue Eng. A*, 2010, **16**, 1703-1716.
22. E. Ruoslahti and M. D. Pierschbacher, *Science*, 1987, **238**, 491-497.
23. E. Ruoslahti, *Annu. Rev. Cell Dev. Biol.*, 1996, **12**, 697-715.

24. U. Hersel, C. Dahmen and H. Kessler, *Biomaterials*, 2003, **24**, 4385-4415.
25. J. A. Rowley, G. Madlambayan and D. J. Mooney, *Biomaterials*, 1999, **20**, 45-53.
26. A. Loebsack, K. Greene, S. Wyatt, C. Culberson, C. Austin, R. Beiler, W. Roland, P. Eiselt, J. A. Rowley, K. Burg, D. J. Mooney, W. Holder and C. Halberstadt, *J. Biomed. Mater. Res. A*, *2001*, **57**, 575-581.
27. N. O. Dhoot, C. A. Tobias, I. Fischer and M. A. Wheatley, *J. Biomed. Mater. Res. A*, 2004, **71**, 191-200.
28. J. W. Lee, Y. J. Park, S. J. Lee, S. K. Lee and K. Y. Lee, *Biomaterials*, 2010, **31**, 5545-5551.
29. S. W. Kang, B. H. Cha, H. Park, K. S. Park, K. Y. Lee and S. H. Lee, *Macromol. Biosci.*, 2011, **11**, 673-679.
30. N. A. Silva, M. J. Cooke, R. Y. Tam, N. Sousa, A. J. Salgado, R. L. Reis and M. S. Shoichet, *Biomaterials*, 2012, **33**, 6345-6354.
31. N. A. Silva, J. Moreira, S. Ribeiro-Samy, E. D. Gomes, R. Y. Tam, M. S. Shoichet, R. L. Reis, N. Sousa and A. J. Salgado, *Biochimie*, 2013, **95**, 2314-2319.
32. L. Doner and D. Douds, *Carbohydr. Res.*, 1995, **273**.
33. L. Doner, *Carbohydr. Polym.*, 1997, **32**, 245-247.
34. D. M. Kirchmajer, B. Steinhoff, H. Warren, R. Clark and M. in het Panhuis, *Carbohydr. Res.*, 2014, **388**, 125-129.
35. T. N. Schumacher and T. J. Tsomides, in *Current protocols in protein science*, Wiley, 2001.
36. E. Ogawa, R. Takahashi, H. Yajima and K. Nishinari, *Biopolymers*, 2005, **79**, 207-217.
37. F. Yang, S. Xia, C. Tan and X. Zhang, *Euro. Food Res. Technol.*, 2013, **237**, 467-479.
38. A. Williams and I. Ibrahim, *J. Am. Chem. Soc.*, 1981, **103**, 7090-7095.
39. R. Timokovich, *Anal. Chem.*, 1977, **143**, 135-143.
40. H. J. Kong, T. Boontheekul and D. J. Mooney, *Proc. Natl. Acad. Sci. U. S. A.*, 2006, **103**, 18534-18539.
41. S. P. Massia and J. A. Hubbell, *J. Cell Biol.* , 1991, **114**, 1089-1100.
42. J. A. Rowley and D. J. Mooney, *J. Biomed. Mater. Res.*, 2002, **60**, 217-223.
43. H. Grasdalen and O. Smidrød, *Carbohydr. Polym.*, 1987, **7**, 371-393.
44. S. Ikeda, Y. Nitta, T. Temsiripong, R. Pongsawatmanit and K. Nishinari, *Food Hydrocolloids*, 2004, **18**, 727-735.
45. M. D. Pierschbacher and E. Ruoslahti, *J. Biol. Chem.*, 1987, **262**, 17294-17298.
46. K.-H. Park, K. Na and K. C. Lee, *J. Biosci. Bioeng.* , 2004, **97**, 207-211.
47. K.-H. Park and K. Yun, *J. Biosci. Bioeng.* , 2004, **97**, 374-377.
48. V. Vogel and M. Sheetz, *Nat. Rev. Mol. Cell. Biol.*, 2006, **7**, 265-275.
49. P. Y. Wang, H. Thissen and W. B. Tsai, *Biotechnol. Bioeng.*, 2012, **109**, 2104-2115.
50. M. Abdul Kafi, W. A. El-Said, T. H. Kim and J. W. Choi, *Biomaterials*, 2012, **33**, 731-739.
51. D. E. Discher, P. Janmey and Y. L. Wang, *Science*, 2005, **310**, 1139-1143.
52. T. Boontheekul, E. E. Hill, H. J. Kong and D. J. Mooney, *Tissue Eng*, 2007, **13**, 1431-1442.
53. D. F. Coutinho, S. V. Sant, H. Shin, J. T. Oliveira, M. E. Gomes, N. M. Neves, A. Khademhosseini and R. L. Reis, *Biomaterials*, 2010, **31**, 7494-7502.
54. H. Lee, S. Fisher, M. S. Kallos and C. J. Hunter, *Journal of biomedical materials research. Part B, Applied biomaterials*, 2011, **98**, 238-245.